

Novel Electronic States in Graphene Ribbons -Competing Spin and Charge Orders-

Atsushi Yamashiro^a, Yukihiro Shimoi^{a,b}, Kikuo Harigaya^{a,b,1},
and Katsunori Wakabayashi^c

^a*Nanotechnology Research Institute, National Institute of Advanced Industrial Science and Technology (AIST),
1-1-1 Umezono, Tsukuba 305-8568, Japan*

^b*Research Consortium for Synthetic Nano-function Materials Project (SYNAF), National Institute of Advanced Industrial
Science and Technology (AIST), 1-1-1 Umezono, Tsukuba 305-8568, Japan*

^c*Department of Quantum Matter Science, Graduate School of Advanced Sciences of Matter (ADSM),
Hiroshima University, Higashi-Hiroshima 739-8530, Japan*

Abstract

In a nanographene ring with zigzag edges, the spin-polarized state and the charge-polarized state are stabilized by the on-site and the nearest neighbor Coulomb repulsions, U and V , respectively, within the extended Hubbard model under the mean field approximation. In a Möbius strip of the nanographene with a zigzag edge, U stabilizes two magnetic states, the domain wall state and the helical state. Both states have ferrimagnetic spins localized along the zigzag edge while the former connects the opposite ferrimagnetic orders resulting in a magnetic frustration forced by the topology and the latter rotates the ferrimagnetic spins uniformly to circumvent the frustration. The helical state is lower in energy than the domain wall state. On the other hand, V stabilizes another domain wall state connecting the opposite charge orders.

Key words: nanographite, edge state, Möbius strip, helical magnetism, domain wall, extended Hubbard model
PACS: 71.10.Hf, 73.22.-f, 73.20.At, 75.75.+a

1. Introduction

Nanoscale materials are strongly affected by their geometries. Carbon nanotubes behave as semiconductor or metal depending on the diameter and the chirality. They opened a new field in fundamental science and have become important materials for nanotechnology devices[1,2,3]. Nanographene ribbons, nanoscale graphite ribbons, also show strikingly different characters depending on the shapes of their

peripheral edges[4,5]. The nanographene ribbon with *zigzag* edges (zigzag ribbon) has the peculiar non-bonding molecular orbitals localized mainly along the zigzag edges (edge states), which cause a sharp peak in the density of states at the Fermi energy, while such states are completely absent in the ribbon with *armchair* edges. Moreover, zigzag ribbons will show rich natures due to the competing spin and charge orders: the introduction of the on-site Coulomb repulsion U under the mean field approximation induces the Fermi-instability of the edge states and results in the spin-polarized (SP) states with the opposite fer-

¹ Corresponding author. E-mail: k.harigaya@aist.go.jp

rimagnetic orders localized along the zigzag edges[4]; On the other hand, the nearest neighbor Coulomb repulsion V induces another Fermi-instability and results in a novel ferroelectrically charge-polarized (CP) state with the unlike charges localized along the zigzag edges and competes with the SP state[6]. Recently, microscopic Möbius strips of NbSe₃ were synthesized [7] and stimulated theoretical studies[5,8,9].

A Möbius strip has unique topological natures different from a ring; the former has only one side and one edge while the latter has two sides and two edges. Then, how such an exotic topology affects the electronic states in nanographene? This is the question that we study here.

In this paper we demonstrate that the Möbius strip has both the SP domain wall (SP-DW) state[5] and the helical state due to U . We also show that V stabilizes the novel domain wall state connecting the opposite charge orders of the CP state (CP-DW).

2. Model and Methods

Figure 1 illustrates the geometry of a zigzag ribbon with an inversion symmetry to make a Möbius strip or a ring. N and L are the width and length of the ribbon. We consider the case both N and L to be even. Note that the twofold coordinated sites locate only at the zigzag edges, PR and QS, where the edge states are mainly localized. Since the zigzag ribbon is bipartite, A and B sites are assigned by black and white circles, respectively. The Möbius strip is obtained by twisting one end of the ribbon, e.g., PQ and joining the ends so that the P site is connected with the S site and the Q site is connected with the R site, defining the Möbius

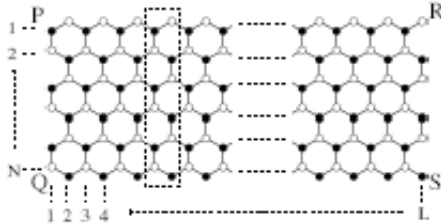


Fig. 1. The schematic structure of a bipartite nanographene ribbon with zigzag edges to make a non-bipartite Möbius strip or a bipartite ring; \bullet (\circ), A (B) site in the bipartite lattice. Dashed rectangle denotes a unit cell in a ring.

boundary condition.

Note that both the P and S sites belong to A sublattice while both the Q and R sites belong to B sublattice. Since the Möbius boundary condition forces to connect the same sublattice, the Möbius strip is not bipartite, while the periodic boundary condition keeps the system bipartite.

We treat a half-filled π electron system on the zigzag ribbon with the extended Hubbard Hamiltonian,

$$H_{EH} = -t \sum_{\langle i,j \rangle, s} (c_{i,s}^\dagger c_{j,s} + \text{H.c.}) + U \sum_i (n_{i,\uparrow} - \frac{1}{2})(n_{i,\downarrow} - \frac{1}{2}) + V \sum_{\langle i,j \rangle} (n_i - 1)(n_j - 1). \quad (1)$$

Here, $\langle i, j \rangle$ denotes a pair of neighboring carbon sites and $-t$ is the transfer integral between them. $c_{i,s}^\dagger$ creates a π electron with spin s on the i -th site and $c_{i,s}$ annihilates the one. $n_{i,s}$ is the corresponding number operator, and $n_i = \sum_s n_{i,s}$.

To study the possibility of the helical state, we gen-

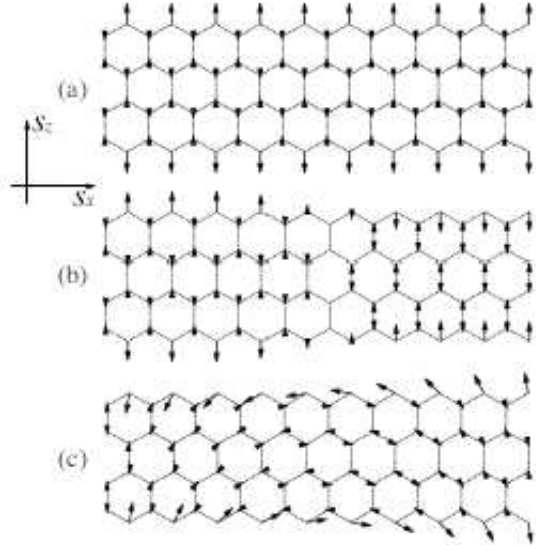


Fig. 2. Spin density distributions of (a) the spin-polarized (SP) state in a ring, (b) the SP domain wall (SP-DW) state and (c) helical states in a Möbius strip with $N \times L = 4 \times 20$ sites for $U = t$ and $V = 0$. Arrows represent spins of π electrons. In (a) and (b), only z component of spin densities $s_{i,z}$ is finite: In (c), y component $s_{i,y}$ is zero.

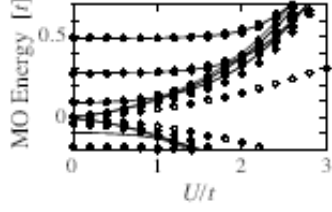


Fig. 3. U dependences of the MO energies of the SP (solid line), SP-DW (○) and helical (●) states for $V = 0$.

eralized the unrestricted Hartree-Fock approximation to set a two body operator as [10],

$$\begin{aligned}
 & \hat{c}_{i,\uparrow}^\dagger \hat{c}_{i,\uparrow} \hat{c}_{i,\downarrow}^\dagger \hat{c}_{i,\downarrow} \\
 \equiv & \langle \hat{c}_{i,\uparrow}^\dagger \hat{c}_{i,\uparrow} \rangle \langle \hat{c}_{i,\downarrow}^\dagger \hat{c}_{i,\downarrow} \rangle + \langle \hat{c}_{i,\uparrow}^\dagger \hat{c}_{i,\uparrow} \rangle \langle \hat{c}_{i,\downarrow}^\dagger \hat{c}_{i,\downarrow} \rangle \\
 - & \langle \hat{c}_{i,\uparrow}^\dagger \hat{c}_{i,\downarrow} \rangle \langle \hat{c}_{i,\downarrow}^\dagger \hat{c}_{i,\uparrow} \rangle - \langle \hat{c}_{i,\uparrow}^\dagger \hat{c}_{i,\downarrow} \rangle \langle \hat{c}_{i,\downarrow}^\dagger \hat{c}_{i,\uparrow} \rangle \\
 - & \langle \hat{c}_{i,\uparrow}^\dagger \hat{c}_{i,\uparrow} \rangle \langle \hat{c}_{i,\downarrow}^\dagger \hat{c}_{i,\downarrow} \rangle + \langle \hat{c}_{i,\uparrow}^\dagger \hat{c}_{i,\downarrow} \rangle \langle \hat{c}_{i,\downarrow}^\dagger \hat{c}_{i,\uparrow} \rangle. \quad (2)
 \end{aligned}$$

The $u(=x, y, z)$ component of the spin density and the charge density at i -th site are given by $s_{i,u} = \sum_{\alpha,\beta} \langle \hat{c}_{i,\alpha}^\dagger (\sigma_u)_{\alpha\beta} \hat{c}_{i,\beta} \rangle / 2$ and $d_i = 1 - \langle n_i \rangle$, respectively, where σ_u is the Pauli matrix.

3. Results and Discussions

Figure 2 shows spin density distributions of (a) the SP state in a ring, and the (b) SP-DW and (c) helical states in a Möbius strip with $N \times L = 4 \times 20$ carbon sites for $U = t$ and $V = 0$. In the SP state, the up- and down-spin ferrimagnetic orders appear along the upper and lower zigzag edges, respectively, because the spin-density-wave like spin-orientation order is stabilized by U in the bipartite system with the edge states at twofold sites [4]. The Möbius boundary condition forces to connect the opposite ferrimagnetic orders along the zigzag edge and causes the magnetic frustration. It allows the SP-DW state with the opposite ferrimagnetic orders connected by the interface where the magnitudes of spins are suppressed to reduce the frustration[5]. On the other hand, the helical state keeps the magnitudes of spins along the zigzag edge with the ferrimagnetic feature in a unit cell. In this state, the directions of spins at twofold sites rotate uniformly along the zigzag edge to circumvent the magnetic frustration due to the Möbius boundary condition. The spin rotates by 2π in the $s_x s_z$ plane dur-

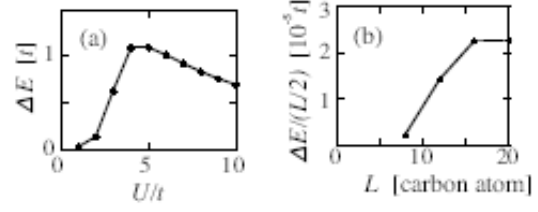


Fig. 4. (a) U dependence of the energy difference $\Delta E = E_{\text{SP-DW}} - E_{\text{helical}}$ for the system with 4×40 sites and $V = 0$, where $E_{\text{SP-DW}}$ and E_{helical} are the energies of the SP-DW and helical states, respectively. (b) Dependence of ΔE per unit cell on the ribbon length L for $U = t$, $V = 0$ and $N = 4$.

ing the travel along the zigzag edge to return to the starting point, showing the helical ferrimagnetic order. Therefore, the SP-DW and helical states satisfy the constraint of the Möbius boundary condition connecting the opposite zigzag edges of the ribbon, i.e., the opposite ferrimagnetic domains in the SP state. A transformation of all spins in the helical state under an Euler angle rotation in the spin space causes another degenerate helical state, since the spin space is isotropic in this model. Total magnetization are zero in the SP-DW and helical states.

In the case of much larger U ($\sim 10t$), the magnitudes of spin densities become almost the same at all sites in the SP and helical states as well as in each ferrimagnetic domain of the SP-DW state: the ferrimagnetic feature turns into the antiferromagnetic one with increasing U .

Figure 3 shows the U dependences of the molecular orbital (MO) energies around the Fermi level in the SP, SP-DW and helical states for the system with $N \times L = 4 \times 40$ sites. In the SP state, U opens the energy gap between the degenerate edge states at the Fermi energy, while in the SP-DW state the frontier orbitals remain inside the gap [5] similar to the soliton state in polyacetylene [11]. On the other hand, in the helical state the frontier orbitals behave more similarly to that in the SP state than in the SP-DW state. This is because the variation of the spin direction in the helical state is extended over the system. In the shorter ribbon with $N \times L = 4 \times 20$, the difference between their behaviors in the SP-DW and helical states is not so appreciable because a half pitch L in the helical state is closer to the size of the interface in the SP-DW state.

For $U > 0$, the helical state is lower in energy than the SP-DW state, as shown in Fig. 4 (a). This is consis-

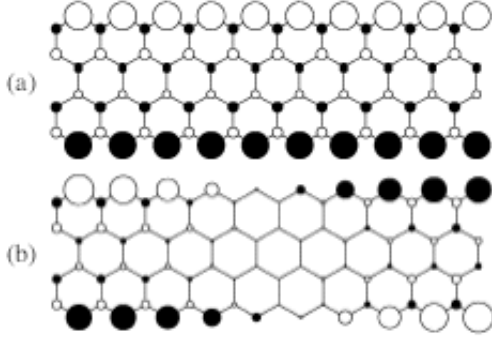


Fig. 5. Charge density, d_i , distribution of (a) the charge-polarized (CP) state in a zigzag ring and (b) the domain wall state connecting the opposite charge orders of the CP state in a Möbius strip for $U = 0.2t$ and $V = 0.4t$; \bullet (\circ), positive (negative) charge densities. The radius of each circle denotes the magnitude of the charge density; the maximal ones are 0.23 in (a) and 0.24 in (b). The system sizes are $N \times L = 4 \times 20$ sites.

tent with the MO's behavior shown in Fig. 3: the wider gap and the enhanced decrease in the occupied MO energies in the helical states than in the SP-DW states. Figure 4 (b) shows that the energy difference per unit cell is smaller in the shorter ribbon, as L approaches the size of the interface in the SP-DW state.

We recently reported that V stabilizes the novel CP state with a finite electric dipole moment under periodic boundary condition[6]. Figure 5 (a) shows the charge density distribution of this state for $U = 0.2t$ and $V = 0.4t$. The positive and negative charges are localized along the lower and upper zigzag edges, respectively, due to V and they form a finite electric dipole moment pointing from the upper edge to the lower edge. Net charge along each zigzag edge arises from much larger charge density at twofold sites than at threefold sites due to the edge states. The magnitude of the electric dipole moment per unit cell is 6.2 Debye in the parameters. This exotic electric dipole moment is induced by V and breaks the inversion symmetry of the system. The CP state competes with the SP state.

In a Möbius strip, corresponding domain wall state, CP-DW state, is stabilized as shown in Fig. 5 (b). It connects the opposite charge orders of the CP state. The Möbius boundary condition allows only the CP-DW state in this case since charge is a scalar, while it allows the SP-DW and helical states in the spin ordered case since spin is a vector. The phase diagram for their competition in the U - V space will be reported

elsewhere.

4. Conclusion

In summary, we demonstrated that a Möbius strip of nanographene with a zigzag edge has the spin-polarized domain wall state and the helical ferrimagnetic state caused by the on-site Coulomb repulsion within the extended-Hubbard model under the mean field approximation and the former is lower in energy than the latter. It also has the charge-polarized domain wall state stabilized by the nearest neighbor Coulomb repulsion which connects the opposite charge orders.

Acknowledgements This work has been supported partly by Special Coordination Funds for Promoting Science and Technology and by NEDO under the Nanotechnology Materials Program. One of us (A. Y.) thanks all the members in his laboratory for helpful discussions and supports.

References

- [1] S. Iijima, *Nature* **354**, 56 (1991).
- [2] M. S. Dresselhaus, G. Dresselhaus, and P. C. Eklund, *Science of Fullerenes and Carbon Nanotubes*, (Academic Press, San Diego, 1996).
- [3] R. Saito, G. Dresselhaus, and M. S. Dresselhaus, *Physical Properties of Carbon Nanotubes*, (Imperial College Press, London, 1998).
- [4] M. Fujita, K. Wakabayashi, K. Nakada, and K. Kusakabe, *J. Phys. Soc. Jpn.* **65**, 1920 (1996).
- [5] K. Wakabayashi and K. Harigaya, *J. Phys. Soc. Jpn.* **72**, 998 (2003).
- [6] A. Yamashiro, Y. Shimoi, K. Harigaya, and K. Wakabayashi, submitted.
- [7] S. Tanda, T. Tsuneta, Y. Okajima, K. Inagaki, K. Yamaya, and N. Hatakenaka, *Nature* **417**, 397 (2002).
- [8] M. Hayashi and H. Ebisawa, *J. Phys. Soc. Jpn.* **70**, 3495 (2001).
- [9] K. Yakubo, Y. Avishai, and D. Cohen, *Phys. Rev. B* **67**, 125319 (2003).

- [10] M. Fujita, M. Ichimura, and K. Nakao, J. Phys. Soc. Jpn. **60**, 2831 (1991).
- [11] A. J. Heeger, S. Kivelson, J. R. Schrieffer, and W. P. Su, Rev. Mod. Phys. **60**, 781 (1998).